SO$_2$ noontime peak phenomenon in the North China Plain

W. Y. Xu[1], C. S. Zhao[1,*], L. Ran[2], W. L. Lin[3,4], P. Yan[3,4], X. B. Xu[3]

[1]{Department of Atmospheric and Oceanic Sciences, School of Physics, Peking University, Beijing, China}

[2]{Key Laboratory of Middle Atmosphere and Global Environment Observation, Institute of Atmospheric Physics, Chinese Academy of Sciences, Beijing, China}

[3]{Key Laboratory for Atmospheric Chemistry, Institute of Atmospheric Composition, Chinese Academy of Meteorological Sciences, Beijing, China}

[4]{Meteorological Observation Center, China Meteorological Administration, Beijing, China}

* Correspondence to: C. S. Zhao (zcs@pku.edu.cn)

Abstract

Frequent SO$_2$ noontime peak phenomenon was discovered in a detailed analysis on the SO$_2$ concentrations in the North China Plain (NCP). The possible causes and their contributions are analysed. The impacts of such a phenomenon on the sulphur cycle were studied and the implications of the phenomenon for atmospheric chemistry, cloud physics and climate were discussed. Different from the common SO$_2$ diurnal patterns with high nighttime concentrations, NCP witnessed high frequencies of SO$_2$ noontime peaks, with an occurrence frequency of 50-72% at the four stations. Down-mixing of elevated pollution layers, plume transport processes, mountain-valley-winds and fog/high RH haze events were the possible causes. The contribution of each process varies from each other and from station to station, however, neither of those four processes can be neglected. SO$_2$ peaks occurring during noontime instead of nighttime will lead to a 13-35% increase in sulphur dry deposition, 9-23% increase in gas phase oxidation and 8-33% increase in aqueous phase conversions, which will increase the hygroscopicity and the light scattering of aerosols, thus having important impacts on atmospheric chemistry, cloud physics and climate.

1 Introduction

High emissions and concentrations of sulphur dioxide (SO_2) have been observed in the North China Plain (NCP) (Lin et al., 2012;Xu et al., 2011b;Zhao et al., 2013), which exerts great impacts on aerosol hygroscopicity and cloud physics (Liu et al., 2011). Yet, the special topography, emission distribution and meteorological conditions in the NCP have complicated the variation of SO_2 concentrations.

The diurnal variation of primary gas pollutants in polluted regions are typically characterized by morning and evening peaks, due to both the diurnal variations of the planetary boundary layer height (PBLH), emissions and the diurnal variation in photochemistry (Jacobson, 2002). The SO_2 diurnal variation pattern observed in both the Yangtze-River-Delta region (Wang et al., 2002;Qi et al., 2012) and the Pearl-River-Delta region (Wang et al., 2001), as well as that observed in other parts of the world (Khemani et al., 1987;Psiloglou et al., 2013) seem to mostly comply to this rule, with a few exceptions found by Qi et al. (2012).

The chemical transformation of SO_2 is most rapid during noontime, when the photochemistry is most active and concentrations of oxidants such as the OH radical, H_2O_2 and O_3 are highest (Hua et al., 2008;Ran et al., 2011). OH is the main oxidant for gas phase SO_2 scavenging, while H_2O_2 and O_3 are the major oxidants in aqueous phase SO_2 scavenging processes (Seinfeld and Pandis, 2006). If SO_2 peak values occurred during noontime instead of during nighttime, sulphur conversions would be enhanced, increasing sulphate concentration in aerosols, leading to higher aerosol hygroscopicity and more light scattering.

Adame et al. (2012) reported rare cases of SO_2 peaking during noontime in Central-Southern Spain, which they attributed to transport from industrial regions. Antony Chen et al. (2001) observed a SO_2 noontime peak only in one out of five measurement periods in Maryland (USA), which were attributed to down-mixing from elevated sources. While this phenomenon seems to be a rare case all over world, several sites in the NCP shows long-term averaged diurnal variation patterns with such variation characteristics (Lin et al., 2011;Lin et al., 2009;Lin et al., 2012;Lin et al., 2008). Short-term observations at both rural and urban sites in the NCP also captured such variation patterns (Gao et al., 2013;Wang et al., 2006b). Long-term measurements at rural sites in the Yangtze River Delta region also displayed pre-noon SO_2 peaks that were not in accordance with the diurnal variation pattern of other primary gas

1 pollutants (Ding et al., 2013;Qi et al., 2012), however, observations during shorter campaigns

2 seem to disagree with these results (Wang et al., 2004). Averaged diurnal patterns usually have

3 large standard deviations due to the high seasonal variability of SO_2 and can be significantly

4 influenced by strong pollution episodes. Thus the representativeness of such averaged profiles

5 is unsure and how common such events were, what might have caused them or what the possible

6 impacts such diurnal variation patterns might have is still not clear. The peak occurrence time

7 at the different type of sites differed from each other, the reason behind that still needs to be

8 found.

9

10 In this study, an elaborate investigation into the SO_2 diurnal variation pattern is made based on

11 observations from four stations in the NCP. Possible causes for the noontime peaks and their

12 relative importance are discussed. Finally, the possible impact of such events on the sulphur

13 cycle is investigated and its influence on atmospheric chemistry and climate are pointed out.

14 **2 Data and Methodology**

15 **2.1 Site and Measurements**

16 Measurements of SO_2 and CO (Carbon Monoxide) were carried out at Wuqing meteorological

17 station (WQ, 39°22'58.8"N 117°1'1.2"E, 7.4m a.s.l) in the NCP during the Haze in China

18 (HaChi) campaign (Jul 2009 - Jan 2010). WQ is located in the heart of the plain region and has

19 been proven to be highly representative of the polluted background(Xu et al., 2011a).

20

21 Measurements from Jan 2009 to Jan 2010 at the Shangdianzi site (SDZ, 40.65 °N, 117.12 °E,

22 293.9 m a.s.l.), the China Meteorological Administration site (CMA, 39.95 °N, 116.32 °E,

23 96 m a.s.l.) and the Gucheng site (GCH, 39.13 °N, 115.12 °E, 15.1 m a.s.l.) made by the Chinese

24 Academy of Meteorological Sciences (Lin et al., 2011;Lin et al., 2009;Lin et al., 2012;Lin et

25 al., 2008) were used as references.

26

27 Radiosonde data from Mar 2009 to Feb 2010 measured at the Nanjiao meteorological station

28 (NJ, 39.8 °N, 116.46 °E, 33 m a.s.l.) were used to analyse the temperature inversion within the

29 PBLH to better understand the vertical mixing process. The radiosonde measurements were

30 carried out every day at 8 am. The temperature inversion depth of each day was determined and

31 the occurrence frequencies of different inversion depths were counted for spring (Mar-May

1   2009), summer (Jun-Aug 2009), autumn (Sep-Nov 2009) and winter (Dec 2009-Feb 2010),

2   respectively.

3

4   The locations of the sites as well as the distribution of SO_2 column concentrations retrieved

5   from the Ozone Monitoring Instrument (OMI) on board AURA satellite (OMSO2Readme file,

6   http://so2.gsfc.nasa.gov/Documentation/OMSO2ReleaseDetails_v111_0303.htm) are shown

7   in Figure 1.

8

9   The SO_2 polluted NCP is surrounded in the north by the Yan Mountains and to the west by the

10   Taihang Mountains. The SDZ, CMA and GCH sites are aligned along a northeast – southwest

11   line east to the Taihang Mountains, while WQ is about 80 km to the southeast of the CMA site.

12   The SDZ, CMA, GCH and WQ sites respectively represent the relatively clean background, the

13   polluted urban, rural and suburban area. SO_2 concentrations are high in the south and relatively

14   lower in the north.

15

16   A set of commercial trace gas instruments (Thermo Environmental Instruments Inc., USA C-

17   series) has been used to continuously monitor various trace gases. SO_2 was measured with

18   pulsed UV fluorescence analysers (TE 43CTL) and CO with gas filter correlation analysers (TE

19   48C). Measured gas concentrations were recorded as 1-min average mixing ratios by volume

20   (ppbv), then averaged into 1 hour resolutions. Details on the measurements and data calibration

21   can be found in Lin et al. (2012) and Xu et al. (2011b).

22   **2.2   Determination of SO_2 noon peak phenomenon**

23   Due to the increased emissions, lower boundary layer heights and slower chemical conversions

24   in winter, SO_2 concentrations show significant seasonal variations. In the study of the average

25   SO_2 diurnal pattern, the enhanced signals of wintertime SO_2 data need to be avoided. SO_2 and

26   CO concentrations were divided by the daily maximum value of each day, to acquire the daily

27   normalized diurnal pattern.

28   Afterwards, patterns with peaks only occurring before 9 am or after 4 pm were grouped into the

29   Nighttime-Peak group (group 1), while patterns of peaks only occurring during 9 am to 4 pm

30   were classified into the Noontime-Peak group (group 2). Diurnal patterns with both a noontime

31   and a nighttime peak during the same day were put into the Nighttime & Noontime group (group

1 3). The normalized diurnal variation patterns in each group were averaged and the standard

2 error of the mean ($\text{SEM} = \sigma/\sqrt{n}$) was calculated for each hour of day. The occurrence

3 frequency of each group was calculated for each month of 2009 and for the whole measurement

4 period.

5 ## 2.3 Four possible causes for the SO_2 noon peak phenomenon

6 Four possible causes for the SO_2 noontime peak phenomenon should be evaluated, the down-

7 mixing for elevated SO_2 pollution layers, the transport of plumes, the influence of mountain-

8 valley breezes and the impact of severe haze or fog events. The diurnal SO_2 profiles of group 2

9 and group 3 were analysed together with the according CO, wind, RH and temperature diurnal

10 profiles to determine which of the above four causes has led to the occurrence of the noon peak.

11 Then the contribution of each cause is yielded by dividing the number of noon peak cases

12 caused by a certain factor with the total number of noon peak cases.

13 If the noon peak was caused by the down-mixing of elevated SO_2 pollution layers, the peak

14 should occur during the early noon time (9-12 LT) when the PBL is developing. Thus, cases

15 with SO_2 peaks occurring after the morning peak of CO along with the development of the PBL

16 were filed under the down-mixing case category. The development of the PBL is represented

17 by the increase in surface temperature.

18 CO has a relatively longer lifetime, thus is a very good tracer for pollution plumes. Days with

19 the correlation coefficient between noontime SO_2 and CO reaching a significance level of 95%

20 were categorized into the plume transport case. Averaged correlation coefficients respectively

21 reached 0.81, 0.82, 0.84 and 0.73 in SDZ, CMA, GCH and WQ.

22 Due to the topography of the NCP, all four sites are under the influence of mountain valley

23 circulations, especially the SDZ, CMA and GCH sites. Winds often change from northern winds

24 to southern ones during noontime (Lin et al., 2009;Lin et al., 2012). SO_2 noontime peak cases

25 with the above described change in wind direction and with maximum wind speeds below 7 m s^{-1}

26 were counted into the mountain valley breezes case (Chen, 2009).

27 Severe haze or fog events are characterized by high RH values. For SDZ, GCH and WQ, the

28 fog or severe haze event is defined as a case with RH exceeding 90% for over 5 consecutive

29 hours. Since CMA is located in urban Beijing and the site is surrounded by heat sources, RH

30 measured at CMA seldom reaches 90%. If the RHs at CMA exceed 80% for over 5 consecutive

hours and the other 3 stations simultaneously show RH greater than 90%, then it is believed that CMA is also experiencing a fog or severe haze event.

2.4 Evaluation of the impacts of the SO_2 noon peak phenomenon on the sulphur cycle

To analyse how the SO_2 diurnal variation pattern influences upon the sulphur cycle, the WQ site of the HaChi Campaign has been selected to represent the polluted background of the NCP. Normalized SO_2 diurnal variation patterns, which were already grouped based on Sect. 2.2, were averaged respectively for summer (Jul-Aug), autumn (Sep-Nov) and winter (Dec-Jan). The occurrence frequency of each group in each season is calculated. The average SO_2 daily maximum value of each season, which is 20, 40 and 75 ppbv for summer, autumn and winter, respectively, is multiplied with the average normalized diurnal patterns to yield characteristic SO_2 diurnal concentration variation patterns for the three groups and for each season.

The characteristic SO_2 diurnal concentration variation patterns of the three groups will yield different dry deposition, gas phase oxidation and aqueous phase transformation amounts, which will be compared against each other. The occurrence frequency of the three groups will also be considered to show how the actual diurnal variation pattern influences the sulphur cycle.

2.4.1 The impact on dry deposition

The dry deposition velocity of SO_2 is under the influence of the surface type. Surfaces covered by vegetation usually show high SO_2 deposition rates during noontime and lower ones during nighttime due to transpiration processes (Tsai et al., 2010;Raymond et al., 2004). SO_2 concentration peaking during noontime instead of nighttime would increase SO_2 dry deposition fluxes, leading to increased acid depositions.

To study the impact of the SO_2 diurnal variation pattern on dry deposition fluxes, the diurnal variation of the dry deposition velocity v_d measured by Tsai et al. (2010) is used and the dry deposition flux is calculated by:

$$F = C \cdot v_d, \tag{1}$$

where C is the SO_2 concentration, which will be provided by the characteristic SO_2 diurnal concentration variation pattern. The dry deposition velocity in the NCP is ranges from 0.2-0.8 cm s^{-1}, showing no significant seasonal variations (Pan et al., 2013), which conforms well with the result of Tsai et al. (2010). Thus, it is believed to be appropriate to use the diurnal

pattern measured by Tsai et al. (2010) for the NCP region. The total daily dry deposition flux of group 2 and group 3 is compared against that of group 1. The daily dry deposition flux of the three groups are averaged weighted by the occurrence frequency of those three groups and is also compared against that of group 1. This will show how the SO_2 diurnal variation characteristics in the NCP increase the dry depositions compared to the common nighttime peak pattern observed in other places of the world.

2.4.2 The impact on gaseous oxidation

The NCAR Master Mechanism (NCAR-MM version 2.4) photochemical box model is used to calculate the homogeneous diurnal oxidation process of SO_2 (Madronich, 2006;Madronich and Calvert, 1990). The model is coupled with a Tropospheric Ultraviolet and Visible Radiation (TUV) model (Madronich and Flocke, 1999), which calculates the photolysis rates needed for photolytic reactions. The radiative properties of the 1st Jul 2009, 1st Oct 2009 and 1st Jan 2010 were modelled to represent the summer, autumn and winter cases, respectively.

Detailed oxidation processes of SO_2 with various atmospheric oxidants (e.g. OH, O_3, NO_x and organic radicals) are included in the model. The concentration of O_3 and NO_x are constrained according to the seasonally averaged diurnal profiles measured during the Hachi Summer Campaign, while that of VOCs could only be constrained according to summertime measurements (Ran et al., 2011). To evaluate the sensitivity of the modelling results to the VOCs concentration assumptions, two additional case scenarios with doubled the amount of summer time VOCs accompanied by half the amount of isoprene and with tripled the amount of summer time VOCs accompanied by a third of the amount of isoprene were calculated. SO_2 concentrations are constrained by the characteristic diurnal variation patterns of the three groups for the three seasons. The entrainment, dilution and dilution processes have been turned off to focus on the oxidation process.

The daily gas phase oxidized SO_2 amount of group 2 and group 3 is compared against that of group 1. The daily gas phase oxidized SO_2 amount of the three groups are averaged weighted by the occurrence frequency of those three groups and is also compared against that of group 1.

1   ## 2.4.3   The impact on aqueous oxidation

2   The SO_2 aqueous oxidation process depends on the atmospheric liquid water content (LWC) as

3   well as the concentration of atmospheric oxidants. For the aqueous phase oxidation of SO_2 the

4   most important two oxidants are H_2O_2 and O_3 (Seinfeld and Pandis, 2006).

5   The aqueous phase oxidized SO_2 amount can be estimated with the following two equations:

6    $$\Delta S(IV) = \left(k_1 \, [SO_2 \cdot H_2O] + k_2 \, [HSO_3{}^-] + k_3 \, [SO_3{}^{2-}] \right) \cdot [O_3] \cdot \Delta t \cdot LWC \cdot 10^{-6} \, , \qquad (2)$$

7    $$\Delta S(IV) = \frac{k_4 \, [H^+][HSO_3{}^-]}{1 + k_5 \, [H^+]} \cdot [H_2O_2] \cdot \Delta t \cdot LWC \cdot 10^{-6} \, , \qquad (3)$$

8   where k_1, … , k_5 are 2.4×10^4 mol^{-1} s^{-1}, 3.7×10^5 mol^{-1} s^{-1}, 3.7×10^5 mol^{-1} s^{-1}, 1.5×10^9 mol^{-1} s^{-1},

9   7.5×10^7 mol^{-2} s^{-1}, 13 mol^{-1}, respectively (Seinfeld and Pandis, 2006). The dissolved

10   concentrations of SO_2, O_3 and H_2O_2 can be calculated with the Henry's Law.

11   Atmospheric LWC exists mostly in clouds, which makes the diurnal variation of atmospheric

12   LWC very complicated. For this study, LWC is assumed to be a constant value 0.029 g m^{-3}

13   throughout the day based on the aircraft measurements of clouds over the NCP (Deng et al.,

14   2009). The pH value is fixed to 5.5 (Sun et al., 2010). The diurnal variation O_3 concentration

15   pattern is set according to Sect. 2.4.2. The H_2O_2 diurnal variation pattern shape is adopted from

16   Hua et al. (2008), due to their relatively long measurement period. The daily maximum H_2O_2

17   value during summer is set according to measurements in Beijing (He et al., 2010), while those

18   in autumn and winter are set to 0.9 and 0.3 based on the H_2O_2 concentration ratio of

19   autumn/winter to summer in (Sakugawa et al., 1990). The SO_2 concentration pattern is set

20   according to the characteristic diurnal variation patterns of the three groups for the three seasons.

21   The daily aqueous phase oxidized SO_2 amount of group 2 and group 3 is compared against that

22   of group 1. The occurrence frequency weighting averaged results of the three groups is also

23   compared against that of group 1.

24   It should be noted that, certain uncertainties will be introduced into this estimation by assuming

25   that trace gas concentrations at cloud level are the same as at ground level. However, the

26   uncertainty will be only shown in the absolute aqueous oxidized amount and will not have

27   influences on the inter-comparison between the groups.

28

3 Results and Discussions

## 3.1 SO$_2$ noontime peak phenomenon in the NCP

While the SO$_2$ diurnal variation in other parts of the world were typically characterized by higher values during the night and lower ones during the day, the NCP has revealed inversed SO$_2$ variation characteristics.

Figure 2a-d displays the season-diurnal variation of SO$_2$ concentrations at SDZ, CMA, GCH and WQ, respectively. It can be noted that SO$_2$ concentrations are usually higher in cold seasons, due to enhanced emissions, weakened removal processes and lower PBLH. Significantly elevated SO$_2$ values during noontime throughout all the seasons were found at the GCH and WQ stations (Figure 2c and d). At SDZ, high SO$_2$ concentrations occur during noontime in all seasons, except for the winter season (Figure 2a). At CMA, noontime SO$_2$ peaks could only be observed in spring and autumn, while in winter high SO$_2$ concentrations occur both during early noon and nighttime (Figure 2b).

The SO$_2$ noontime peak seems to be a common phenomenon throughout the NCP region, especially at the WQ and GCH site, at which the measurements are more representative of the regional background pollution. However, how frequent such events occur, what the causes are and what impacts they may have on atmospheric chemistry, cloud physics and climate is still unknown.

For the study of the average diurnal pattern, normalized diurnal patterns were calculated and classified into the Nighttime-Peak group (group 1), the Noontime-Peak group (group 2) and the Nighttime & Noontime group (group 3). The average normalized diurnal variation pattern of

1   each group, the according SEM and the occurrence frequency of each group is displayed in
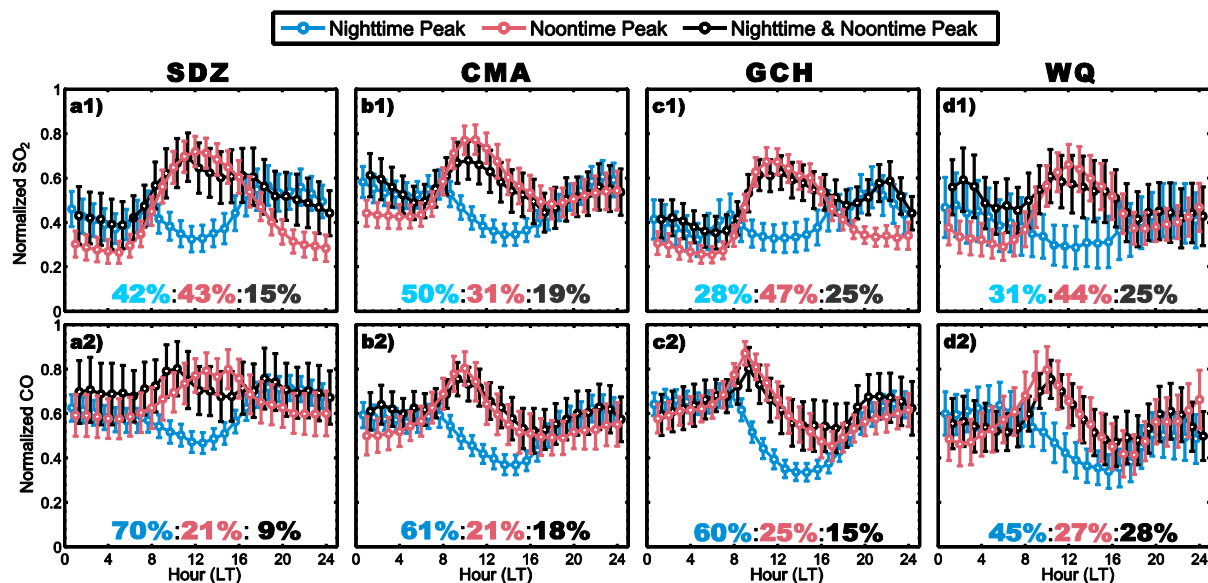
2

3   Figure 3.

4

5   As   depicted   in
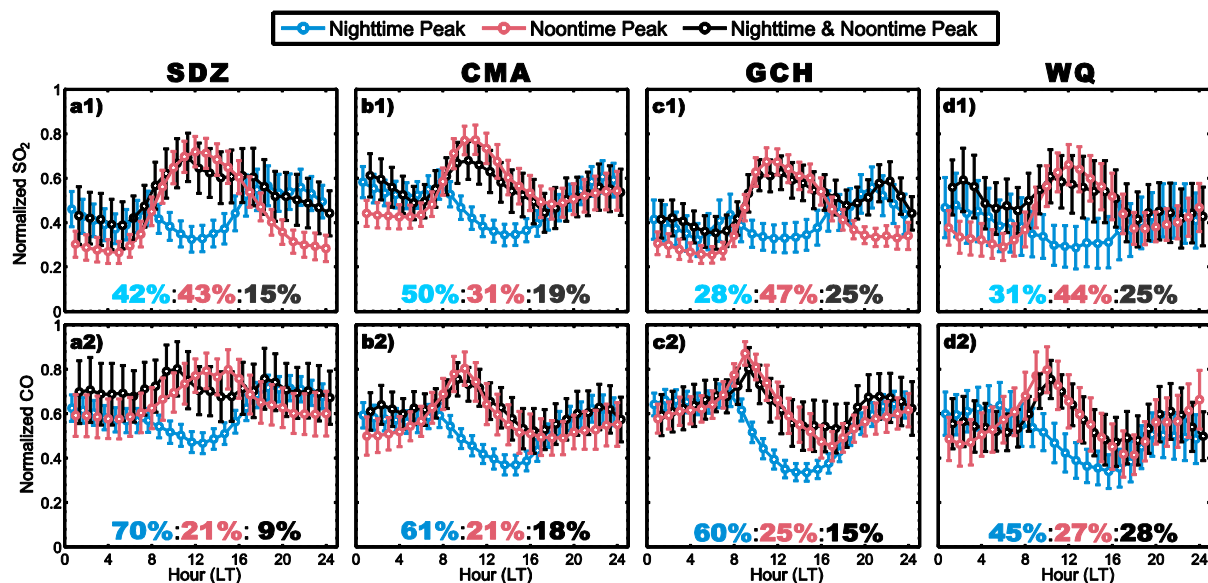
6

7   Figure 3a1-d1, the total SO_2 noontime peak occurrence frequency (group 2 + group 3)

8   respectively reached 58%, 50%, 72% and 69% at the SDZ, CMA, GCH and WQ station. Days

9   with only one noontime peak were more common (SDZ: 43%, CMA: 31%, GCH: 47%, WQ:

10   44%), while cases with both noontime and nighttime peaks also often occurred (SDZ: 15%,

11   CMA: 19%, GCH: 25%, WQ: 25%). At SDZ, GCH and WQ, the average normalized SO_2

12   concentration reaches its peak at 12 am, while at CMA the peak occurs between 10 to 11 am.

The averaged diurnal variation pattern of group 3 show lower peak values than group 2 and the peaks tend to occur 1 hour earlier than in group 2. However, both group 2 and group 3 for SO_2 reveal distinct noontime peaks.

The averaged diurnal patterns of CO for the CMA, GCH and WQ sites resemble each other in shape. The normalized CO concentrations of group 2 and group 3 all show peaks at 9 am, which can also be seen as late morning peaks. At SDZ, the CO peak of group 2 occurs between 12 am to 2 pm, while that of group 3 is also found between 9-10 am. The total noontime peak occurrence frequency of CO for SDZ, CMA, GCH and WQ is 30%, 39%, 40% and 55%, respectively.

The total occurrence frequencies of noontime SO_2 peaks in each month for the four stations are listed in Table 1. Distinctly higher occurrence frequencies during warmer seasons were found in SDZ, while in CMA the occurrence frequencies are high in spring and autumn. Noontime peak occurrence frequencies in GCH show less regular seasonal variations, while those in WQ are relatively lower in summer and higher in autumn and winter.

It can be concluded that, the SO_2 noontime peak phenomenon occurs frequently at the NCP sites, regardless of seasons. The average peak is mostly reached at 12 am. The highest noontime peak occurrence frequencies were found at GCH and WQ, the two sites that are most representative of the background pollution state of the NCP. Only a few CO noontime peaks were found and most of them are late morning peaks.

3.2   Causes for SO_2 noontime peak phenomenon

Different from the SO_2 diurnal patterns in other places of the world, the high SO_2 emissions and concentrations together with the special topography and meteorological characteristics in the NCP have led to a unique noontime peak pattern. The SO_2 noontime peak could be attributed to four possible causes.

PBL mixing is strongest during noontime, during which down-mixing processes of elevated SO_2 polluted layers will be enhanced. Elevated SO_2 pollution layers could have formed through the emission of stacks whose plumes can rise above the surface temperature inversion layer or

through the mountain-chimney-effect (Chen et al., 2009), in which surface SO_2 plumes are inject into the free troposphere through valley winds during the afternoon and transported back to the plain with westerly winds. As is shown in Figure 4, temperature inversions during 08 LT are most common in autumn and winter, with occurrence frequencies exceeding 80% of the days. In spring and summer, over 60% of the days experienced temperature inversions at 08 LT. Inversion depth are typically shallow, with 89%, 98%, 72% and 73% of the days showing inversion layers depths less than 250 m during spring, summer, autumn and winter 2009, respectively. Inversion depth are especially shallow in spring and summer, with over 80 and 96% of the days showing inversion layers below 100 m, respectively. Stacks of industries and power plants are typically 10-240 m high and the higher stacks are emitting a significantly larger amount of SO_2 compared to the smaller stacks (Wang et al., 2006a;Yang et al., 2008;Zhou et al., 2003). Additionally, due to the plume rise process, the effective plume height could be much higher than the stack heights (Slawson and Csanady, 1971). Thus, the frequent occurrence of shallow inversions together with the large amount of SO_2 that is released from higher stacks will favor the formation of elevated SO_2 pollution layers. The average normalized SO_2, CO and temperature profiles that were filed under the down-mixing case category are displayed in Figure 5a1-a4. Down-mixing case samples take up 34%, 30%, 43% and 52% of the noontime peaks at SDZ, CMA, GCH and WQ, respectively (Table 2a).

The transport of SO_2 plumes can result in sudden increases of local SO_2 concentrations. The plume transport process is characterized by the cohesive variation of SO_2 and CO. The average normalized SO_2, CO and temperature profiles in the plume transport case can be seen in Figure 5b1-b4. Although SO_2 shows a peak between 9 and 12 am, the occurrence time of the peaks caused by plume transport processes was rather random. This process respectively explains 21%, 46%, 20% and 30% of the noontime peaks at SDZ, CMA, GCH and WQ (Table 2b). It should be noted that, due to our classification method, cases with SO_2 and CO both having a late morning peak are also included into this category.

Mountain valley circulations lead to diurnal variations in wind directions, thus resulting in a diurnal variation in pollutant transport. Due to the topography of the NCP, all four sites are under the influence of mountain valley circulations, especially the SDZ, CMA and GCH sites. Winds often change from northern winds to southern ones during noontime. Due to the stronger SO_2 emissions and resulting higher concentrations in the southern part of the NCP (Figure 1),

southern winds will aid the transport of polluted air masses to our stations. The average diurnal patterns in the mountain valley breezes case are shown in Figure 5a3-d3. A change in wind direction takes place between 8 am to 12 am, while SO_2 starts increasing before noon and reaches its peak between 12 am and 4 pm at all four stations. As can be seen in Table 2c, the mountain valley breeze factor can respectively explain 40%, 20%, 20% and 6% of the noontime peaks occurring in SDZ, CMA, GCH and WQ. Since SDZ is a relatively clean background site, the mountain-valley breeze will not only cause increasing noontime SO_2 concentrations but also increasing CO concentrations. This explains why only the SDZ site showed noontime CO peaks in
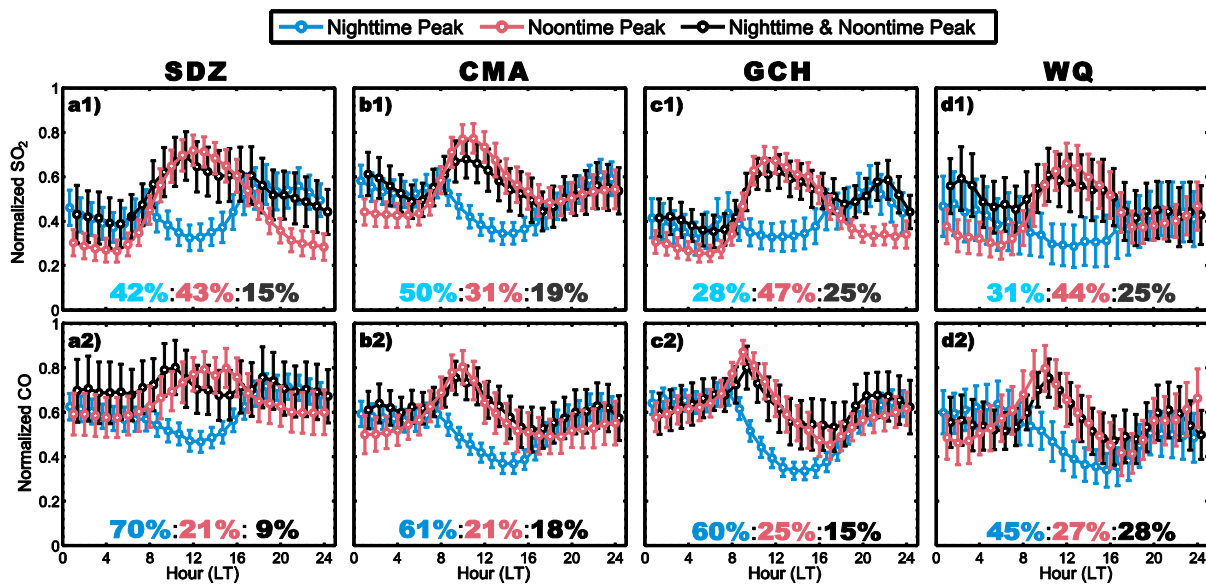
Figure 3.

Aerosol and fog liquid water can serve as an efficient sink for SO_2. SO_2 is a soluble gas, which can be scavenged effectively through aqueous phase reactions in fog or wet aerosol particles (Pandis et al., 1992). Fog and high RH haze events usually occur during nighttime and persist until the temperature rises up in the morning, leading to low nighttime SO_2 concentrations. Additionally, such events are typically characterized by surface temperature inversions, which will prevent the down-mixing of elevated SO_2 emissions (Jacobson, 2002). With the increasing temperature in the morning, the RH will decrease, weakening the SO_2 scavenging process. The temperature inversion will vanish, allowing for the down-mixing of SO_2 from aloft. Averaged normalized SO_2, CO and RH profiles in the fog or severe haze case are shown in Figure 5d1-d4. SO_2 peaks were reached typically between 12 am and 16 pm, depending on how long the

1   fog or high RH event lasted. Such events caused 5%, 4%, 18% and 12% of the noontime peak

2   events at SDZ, CMA, GCH and WQ, respectively.

3

4   **3.3 Impacts of SO₂ noontime peak phenomenon on the sulphur cycle**

5   SO_2 peaks occurring during noontime instead of nighttime might have remarkable impacts on

6   human health, environment and climate. Higher SO_2 concentrations during daytime will not

7   only pose higher health risks for humans, but also change the sulphur cycle.

8   The calculated diurnal dry deposition fluxes based on the diurnal dry deposition velocity in Tsai

9   et al. (2010) and the characteristic SO_2 diurnal variations of the three groups in WQ during

10   autumn are shown in Figure 6. Group 2 and 3 show significantly higher dry deposition fluxes

11   than group1 during 8 am to 6 pm (LT), while for the other time periods the dry deposition fluxes

12   of the three groups are similar to one another. The estimated daily deposition fluxes for summer,

13   winter and autumn in WQ are listed in Table 3. Seasonally, dry deposition fluxes are higher

14   during colder seasons than during warmer ones, due to elevated SO_2 concentrations and due to

15   the fact that seasonal variations in dry deposition rates were not considered. Within the same

16   season, the occurrence time of the SO_2 peak had major impacts on the daily dry deposition

17   fluxes. The results of group 2 show a 22-46% increase in daily dry deposition flux compared to

18   those of group 1, while those of group 3 show a 44-62% increase. Considering the occurrence

19   frequency of the three diurnal patterns, the weighting averaged daily dry deposition fluxes show

20   increases of 13-35% relative to the common nighttime peak case, with the lowest increase

21   occurring during summer and the highest one during autumn.

22   Atmospheric photochemistry is most active during noontime due to favourable radiative

23   conditions. The simulated SO_2 gas phase conversion processes for the three SO_2 diurnal

24   variation patterns in WQ during autumn are displayed in Figure 7. Due to the fact that

25   deposition processes have been turned off in the simulations, S(VI) products will accumulate

26   in the air parcel. Accumulated S(VI) concentrations of group 3 are the highest throughout the

27   day, while that of group 2 exceeds that of group 1 after 10 am. The SO_2 oxidation rates of group

28   2 and 3 during noontime are significantly higher than those of group 1. The simulated daily gas

29   phase SO_2 conversion amount for summer, winter and autumn in WQ are listed in Table 4.

30   Despite the weakened photochemistry during winter, the high SO_2 concentration in winter has

31   led to higher gas phase oxidized SO_2 amounts than in summer. SO_2 noontime peak patterns

14

1 could also increase the daily gas phase oxidized SO_2 amount. The results of group 2 show a 15-
2 26% increase in gas phase oxidized amount compared to those of group 1, while those of group
3 3 show a 28-50% increase. Considering the occurrence frequency of the three diurnal patterns,
4 the weighting averaged gas phase oxidized amounts show increases of 9-23% relative to the
5 common nighttime peak case, with the lowest increase occurring during summer and the highest
6 one in winter. Increased VOCs concentrations during autumn and winter will lead to increased
7 SO_2 oxidized amounts, however, the relative increase of group 2 and group 3 to that of group 1
8 decreases slightly with increasing VOCs concentrations. Overall, the VOCs concentrations
9 have little influence in the inter-comparison between the three groups.

10 Concentrations of atmospheric oxidants that are important in SO_2 aqueous phase reactions also reach their peaks
11 during noontime. Assuming a constant LWC throughout the day and assuming that concentrations near clouds are
12 similar to the surface concentrations, the estimated SO_2 aqueous phase conversion rate for the three SO_2 diurnal
13 variation   patterns   in   WQ   during   autumn   are   displayed
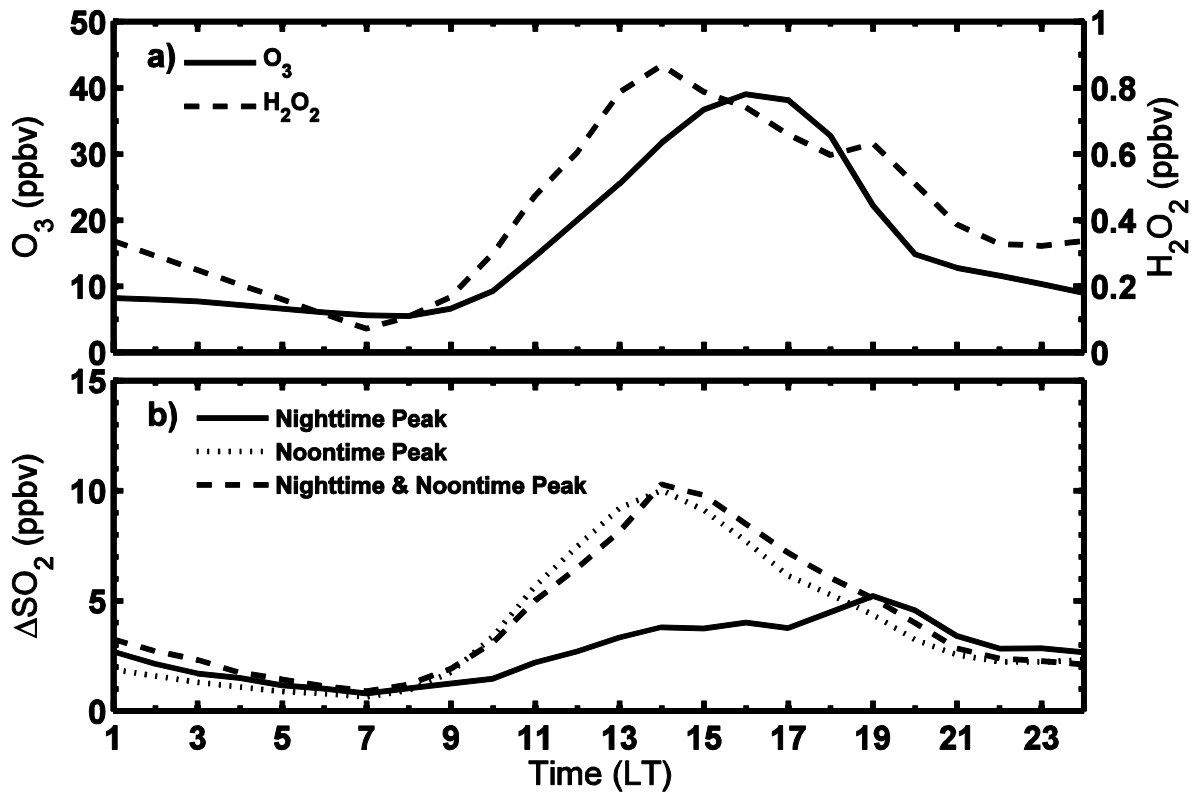
14

15 Figure 8. SO_2 conversion amounts of group 2 and 3 are significantly higher than those of group
16 1 during 8 am to 6 pm, with that of group 2 being highest between 11 am to 4 pm. The simulated
17 daily aqueous phase SO_2 conversion amount for summer, winter and autumn in WQ are listed
18 in Table 5. The aqueous phase scavenged SO_2 amounts during the three seasons are on the same
19 level. The high SO_2 concentrations in winter have been cancelled out by the low concentrations

15

1   in oxidants. The diurnal variation pattern however had much impact on the aqueous phase
2   oxidized SO_2 amount. Compared to group 1, group 2 shows a 13-43% increase in aqueous phase
3   conversion amount, while group 3 shows a 28-61% increase. Considering the occurrence
4   frequency of the three diurnal patterns, the weighting averaged aqueous phase SO_2 conversion
5   amounts show increases of 8-33% relative to the common nighttime peak case, with the lowest
6   increase occurring during summer and the highest one during autumn.

7   In all, compared to the nighttime SO_2 peak case, which was observed all around the world, the
8   NCP experienced enhanced sulphur dry depositions and sulphur to sulphate conversions due to
9   the frequently occurring SO_2 noontime peak phenomenon. More acidic deposition is formed.
10 Aerosols in the NCP will show higher sulphate fractions and become more hygroscopic (Liu et
11 al., 2013). This will promote the light scattering effect of aerosols and thus may have important
12 impacts on regional climate.

13

4   Summary

15 In this paper, a frequently occurring SO_2 noontime peak pattern was found in the NCP. A
16 detailed analysis of this SO_2 diurnal pattern, the causes for such a phenomenon and the potential
17 impacts of the phenomenon on the sulphur cycle were investigated.
18 The total noontime peak occurrence frequency reaches 68%, 50%, 72% and 69% in SDZ, CMA,
19 GCH and WQ, respectively. Down-mixing of elevated pollution layers, plume transport
20 processes, mountain-valley-winds and fog/high RH haze events were the possible causes. The
21 contribution of each process varies from each other and from station to station, which the down-
22 mixing process being the most important process at three out of four stations. However, none
23 of those four processes is negligible. The different occurrence frequencies of noontime peak
24 phenomenon and the different contribution of each process to each site has led to distinct
25 noontime peak occurrence times in the long-term averaged diurnal profiles at the different types
26 of sites.
27 The SO_2 noontime peak phenomenon significantly speeds up the sulphur cycle. Compared to
28 the nighttime SO_2 peak case, which was observed all around the world, WQ respectively
29 experienced 13-35%, 9-23% and 8-33% enhancement in sulphur dry depositions, gas phase
30 oxidations and aqueous phase conversions due to the frequently occurring SO_2 noontime peak
31 phenomenon.

SO$_2$ peaks occurring during noontime instead of nighttime has led to more acidic deposition. Aerosols in the NCP will show higher sulphate fractions and become more hygroscopic. This will promote the light scattering effect of aerosols and thus may have important impacts on regional climate. Higher SO$_2$ concentrations during daytime will also pose higher health risks for human. The potential impacts of such a phenomenon on human health, environment and climate should be studied in detail in the future.

17

References

OMSO2 Release Specific Information: http://so2.gsfc.nasa.gov/Documentation/OMSO2ReleaseDetails_v111_0303.htm, access: 28 March 2013.

Adame, J. A., Notario, A., Villanueva, F., and Albaladejo, J.: Application of cluster analysis to surface ozone, NO_2 and SO_2 daily patterns in an industrial area in Central-Southern Spain measured with a DOAS system, Science of The Total Environment, 429, 281-291, http://dx.doi.org/10.1016/j.scitotenv.2012.04.032, 2012.

Antony Chen, L. W., Doddridge, B. G., Dickerson, R. R., Chow, J. C., Mueller, P. K., Quinn, J., and Butler, W. A.: Seasonal variations in elemental carbon aerosol, carbon monoxide and sulfur dioxide: Implications for sources, Geophysical Research Letters, 28, 1711-1714, 10.1029/2000GL012354, 2001.

Chen, Y.: The impact of local circulation on the dirstribution and transport of atmospheric pollutants in Beijing., M.S. Thesis, Department of Atmospheric and Oceanic Sciences, Peking University, Beijing, 2009.

Chen, Y., Zhao, C., Zhang, Q., Deng, Z., Huang, M., and Ma, X.: Aircraft study of Mountain Chimney Effect of Beijing, China, Journal of Geophysical Research: Atmospheres, 114, D08306, 10.1029/2008JD010610, 2009.

Deng, Z., Zhao, C., Zhang, Q., Huang, M., and Ma, X.: Statistical analysis of microphysical properties and the parameterization of effective radius of warm clouds in Beijing area, Atmospheric Research, 93, 888-896, http://dx.doi.org/10.1016/j.atmosres.2009.04.011, 2009.

Ding, A. J., Fu, C. B., Yang, X. Q., Sun, J. N., Zheng, L. F., Xie, Y. N., Herrmann, E., Nie, W., Petäjä, T., Kerminen, V. M., and Kulmala, M.: Ozone and fine particle in the western Yangtze River Delta: an overview of 1 yr data at the SORPES station, Atmos. Chem. Phys., 13, 5813-5830, 10.5194/acp-13-5813-2013, 2013.

Gao, X., Nie, W., Xue, L., Wang, T., Wang, X., Gao, R., Wang, W., Yuan, C., Gao, J., Ravi, K. P., Wang, J., and Zhang, Q.: Highly Time-Resolved Measurements of Secondary Ions in PM2.5 during the 2008 Beijing Olympics: The Impacts of Control Measures and Regional Transport, Aerosol and Air Quality Research, 13, 367-376, 10.4209/aaqr.2012.04.0083, 2013.

He, S. Z., Chen, Z. M., Zhang, X., Zhao, Y., Huang, D. M., Zhao, J. N., Zhu, T., Hu, M., and Zeng, L. M.: Measurement of atmospheric hydrogen peroxide and organic peroxides in Beijing before and during the 2008 Olympic Games: Chemical and physical factors influencing their concentrations, Journal of Geophysical Research: Atmospheres, 115, D17307, 10.1029/2009JD013544, 2010.

Hua, W., Chen, Z. M., Jie, C. Y., Kondo, Y., Hofzumahaus, A., Takegawa, N., Chang, C. C., Lu, K. D., Miyazaki, Y., Kita, K., Wang, H. L., Zhang, Y. H., and Hu, M.: Atmospheric hydrogen peroxide and organic hydroperoxides during PRIDE-PRD'06, China: their concentration, formation mechanism and contribution to secondary aerosols, Atmos. Chem. Phys., 8, 6755-6773, 10.5194/acp-8-6755-2008, 2008.

Jacobson, M. Z.: Atmospheric Pollution: History, Science, and Regulation, Cambridge University Press, Cambridge 2002.

Khemani, L. T., Momin, G. A., and Singh, G.: Variations in trace gas concentrations in different environments in India, PAGEOPH, 125, 167-181, 10.1007/BF00878620, 1987.

Lin, W., Xu, X., Zhang, X., and Tang, J.: Contributions of pollutants from North China Plain to surface ozone at the Shangdianzi GAW Station, Atmos. Chem. Phys., 8, 5889-5898, 10.5194/acp-8-5889-2008, 2008.

Lin, W., Xu, X., Ge, B., and Zhang, X.: Characteristics of gaseous pollutants at Gucheng, a rural site southwest of Beijing, J. Geophys. Res., 114, D00G14, 10.1029/2008jd010339, 2009.

Lin, W., Xu, X., Ge, B., and Liu, X.: Gaseous pollutants in Beijing urban area during the heating period 2007–2008: variability, sources, meteorological, and chemical impacts, Atmos. Chem. Phys., 11, 8157-8170, 10.5194/acp-11-8157-2011, 2011.

Lin, W., Xu, X., Ma, Z., Zhao, H., Liu, X., and Wang, Y.: Characteristics and recent trends of sulfur dioxide at urban, rural, and background sites in North China: Effectiveness of control measures, Journal of Environmental Sciences, 24, 34-49, http://dx.doi.org/10.1016/S1001-0742(11)60727-4, 2012.

Liu, H. J., Zhao, C. S., Nekat, B., Ma, N., Wiedensohler, A., van Pinxteren, D., Spindler, G., Müller, K., and Herrmann, H.: Aerosol hygroscopicity derived from size-segregated chemical composition and its parameterization in the North China Plain, Atmos. Chem. Phys. Discuss., 13, 20885-20922, 10.5194/acpd-13-20885-2013, 2013.

Liu, P. F., Zhao, C. S., Göbel, T., Hallbauer, E., Nowak, A., Ran, L., Xu, W. Y., Deng, Z. Z., Ma, N., Mildenberger, K., Henning, S., Stratmann, F., and Wiedensohler, A.: Hygroscopic properties of aerosol particles at high relative humidity and their diurnal variations in the North China Plain, Atmos. Chem. Phys., 11, 3479-3494, 10.5194/acp-11-3479-2011, 2011.

Madronich, S., and Calvert, J. G.: Permutation reactions of organic peroxy radicals in the troposphere, Journal of Geophysical Research: Atmospheres, 95, 5697-5715, 10.1029/JD095iD05p05697, 1990.

Madronich, S., and Flocke, S.: The role of solar radiation in atmospheric chemistry, in: The Handbook of Environmental Chemistry, edited by: Boule, P., Springer-Verlag Berlin Heidelberg, 1-26, 1999.

Madronich, S.: Chemical evolution of gaseous air pollutants down-wind of tropical megacities: Mexico City case study, Atmospheric Environment, 40, 6012-6018, http://dx.doi.org/10.1016/j.atmosenv.2005.08.047, 2006.

Pan, Y. P., Wang, Y. S., Tang, G. Q., and Wu, D.: Spatial distribution and temporal variations of atmospheric sulfur deposition in Northern China: insights into the potential acidification risks, Atmos. Chem. Phys., 13, 1675-1688, 10.5194/acp-13-1675-2013, 2013.

Pandis, S. N., Seinfeld, J. H., and Pilinis, C.: Heterogeneous sulfate production in an urban fog, Atmospheric Environment. Part A. General Topics, 26, 2509-2522, http://dx.doi.org/10.1016/0960-1686(92)90103-R, 1992.

Psiloglou, B., Larissi, I., Petrakis, M., Paliatsos, A., Antoniou, A., and Viras, L.: Case studies on summertime measurements of O_3, NO_2, and SO_2 with a DOAS system in an urban semi-industrial region in Athens, Greece, Environ Monit Assess, 185, 7763-7774, 10.1007/s10661-013-3134-2, 2013.

Qi, H., Lin, W., Xu, X., Yu, X., and Ma, Q.: Significant downward trend of SO_2 observed from 2005 to 2010 at a background station in the Yangtze Delta region, China, Sci. China Chem., 55, 1451-1458, 10.1007/s11426-012-4524-y, 2012.

Ran, L., Zhao, C. S., Xu, W. Y., Lu, X. Q., Han, M., Lin, W. L., Yan, P., Xu, X. B., Deng, Z. Z., Ma, N., Liu, P. F., Yu, J., Liang, W. D., and Chen, L. L.: VOC reactivity and its effect on

ozone production during the HaChi summer campaign, Atmos. Chem. Phys., 11, 4657-4667, 10.5194/acp-11-4657-2011, 2011.

Raymond, H. A., Yi, S.-M., Moumen, N., Han, Y., and Holsen, T. M.: Quantifying the dry deposition of reactive nitrogen and sulfur containing species in remote areas using a surrogate surface analysis approach, Atmospheric Environment, 38, 2687-2697, http://dx.doi.org/10.1016/j.atmosenv.2004.02.011, 2004.

Sakugawa, H., Tsai, W., Kaplan, I. R., and Cohen, Y.: Factors controlling the photochemical generation of gaseous H_2O_2 in the Los Angeles atmosphere, Geophysical Research Letters, 17, 93-96, 10.1029/GL017i001p00093, 1990.

Slawson, P., and Csanady, G.: The effect of atmospheric conditions on plume rise, Journal of Fluid Mechanics, 47, 33-49, 1971.

Sun, M., Wang, Y., Wang, T., Fan, S., Wang, W., Li, P., Guo, J., and Li, Y.: Cloud and the corresponding precipitation chemistry in south China: Water-soluble components and pollution transport, Journal of Geophysical Research: Atmospheres, 115, D22303, 10.1029/2010JD014315, 2010.

Tsai, J.-L., Chen, C.-L., Tsuang, B.-J., Kuo, P.-H., Tseng, K.-H., Hsu, T.-F., Sheu, B.-H., Liu, C.-P., and Hsueh, M.-T.: Observation of SO_2 dry deposition velocity at a high elevation flux tower over an evergreen broadleaf forest in Central Taiwan, Atmospheric Environment, 44, 1011-1019, 10.1016/j.atmosenv.2009.12.022, 2010.

Wang, S., Hao, J., Ho, M. S., Li, J., and Lu, Y.: Intake fractions of industrial air pollutants in China: Estimation and application, Science of The Total Environment, 354, 127-141, http://dx.doi.org/10.1016/j.scitotenv.2005.01.045, 2006a.

Wang, T., Cheung, V. T. F., Lam, K. S., Kok, G. L., and Harris, J. M.: The characteristics of ozone and related compounds in the boundary layer of the South China coast: temporal and vertical variations during autumn season, Atmospheric Environment, 35, 2735-2746, 10.1016/s1352-2310(00)00411-8, 2001.

Wang, T., Cheung, T. F., Li, Y. S., Yu, X. M., and Blake, D. R.: Emission characteristics of CO, NO_x, SO_2 and indications of biomass burning observed at a rural site in eastern China, J. Geophys. Res., 107, 4157, 10.1029/2001jd000724, 2002.

Wang, T., Wong, C. H., Cheung, T. F., Blake, D. R., Arimoto, R., Baumann, K., Tang, J., Ding, G. A., Yu, X. M., Li, Y. S., Streets, D. G., and Simpson, I. J.: Relationships of trace gases and aerosols and the emission characteristics at Lin'an, a rural site in eastern China, during spring 2001, J. Geophys. Res., 109, D19S05, 10.1029/2003JD004119, 2004.

Wang, T., Ding, A., Gao, J., and Wu, W. S.: Strong ozone production in urban plumes from Beijing, China, Geophys. Res. Lett., 33, L21806, 10.1029/2006gl027689, 2006b.

Xu, W., Zhao, C., Ran, L., Deng, Z., Liu, P., Ma, N., Lin, W., Xu, X., and Yan, P.: Characteristics of Pollutants at a Suburban Site in the North China Plain and estimated regional Emissions and Contributions, AGU Fall Meeting Abstracts, 1, 0053, 2011a.

Xu, W. Y., Zhao, C. S., Ran, L., Deng, Z. Z., Liu, P. F., Ma, N., Lin, W. L., Xu, X. B., Yan, P., He, X., Yu, J., Liang, W. D., and Chen, L. L.: Characteristics of pollutants and their correlation to meteorological conditions at a suburban site in the North China Plain, Atmos. Chem. Phys., 11, 4353-4369, 10.5194/acp-11-4353-2011, 2011b.

Yang, D., Wang, Z., and Zhang, R.: Estimating Air Quality Impacts of Elevated Point Source Emissions in Chongqing, China, Aerosol and Air Quality Research, 8, 279-294, 10.4209/aaqr.2008.02.0005, 2008.

Zhao, P. S., Dong, F., He, D., Zhao, X. J., Zhang, X. L., Zhang, W. Z., Yao, Q., and Liu, H. Y.: Characteristics of concentrations and chemical compositions for PM2.5 in the region of Beijing, Tianjin, and Hebei, China, Atmos. Chem. Phys., 13, 4631-4644, 10.5194/acp-13-4631-2013, 2013.

Zhou, Y., Levy, J. I., Hammitt, J. K., and Evans, J. S.: Estimating population exposure to power plant emissions using CALPUFF: a case study in Beijing, China, Atmospheric Environment, 37, 815-826, http://dx.doi.org/10.1016/S1352-2310(02)00937-8, 2003.

1   Table 1 Seasonal variation of noontime peak occurrence frequency

Month	Noontime Peak Occurrence Frequency (%)			
	SDZ	CMA	GCH	WQ
Jan	39	33	71	-
Feb	32	29	89	-
Mar	26	39	65	-
Apr	33	70	70	-
May	42	47	52	-
Jun	60	50	50	-
Jul	67	32	81	40
Aug	71	55	68	48
Sep	73	67	63	69
Oct	77	58	71	62
Nov	53	52	57	62
Dec	37	16	65	64

2

3

1   Table 2 SO$_2$ noontime peak occurrence frequency and the fraction of noontime peaks caused

2   by a) down-mixing due to PBL processes, b) plume transport, c) mountain valley breezes and

3   d) fog or severe haze events

Station	SDZ	CMA	GCH	WQ
Total Sample Count	356	374	395	180
Noontime Peak Sample Count (Occurrence Frequency)				
	179(50%)	165(44%)	269(68%)	105(58%)
a) Down-mixing caused Noontime Peak Sample Count				
	60 (34%)	50 (30%)	117 (43%)	55(52%)
b) Plume transport caused Noontime Peak Sample Count				
	38 (21%)	76 (46%)	53 (20%)	31(30%)
c) Mountain Valley Breeze caused Noontime Peak Sample Count				
	72 (40%)	33(20%)	53 (20%)	6 (6%)
d) Fog or severe haze events caused Noontime Peak Sample Count				
	9 (5%)	6 (4%)	49 (18%)	13 (12%)

4

5

1   Table 3 Estimated SO_2 dry deposition flux for the three different SO_2 diurnal variation patterns,

2   the occurrence frequency (of the three groups) weighting averaged value and the relative

3   increase compared to the nighttime peak case.

Case	SO_2 dry deposition flux (g m^{-2} day^{-1}) [Increase relative to nighttime peak case (%)]		
	Summer	Autumn	Winter
Nighttime Peak	0.0065	0.014	0.028
Noontime Peak	0.0079 (22%)	0.020 (46%)	0.035 (27%)
Nighttime+Noontime Peak	0.0093 (44%)	0.022 (58%)	0.045 (62%)
Weighting average	0.0073 (13%)	0.019 (35%)	0.035 (28%)

4

1

2 Table 4 Simulated SO_2 gaseous oxidation amount for the three different SO_2 diurnal variation

3 patterns, the occurrence frequency (of the three groups) weighting averaged value and the

4 relative increase compared to the nighttime peak case. Case1, Case2 and Case3 respectively

5 represent cases using summertime VOCs concentrations, doubled summertime VOCs

6 concentrations with half of the summertime isoprene concentrations and tripled summertime

7 VOCs concentrations with a third of the summertime isoprene concentrations.

| Case	SO_2 gaseous oxidized amount (ppbv day^{-1}) [Increase relative to nighttime peak case (%)]						
	summer	autumn			winter		
	Case1	Case1	Case2	Case3	Case1	Case2	Case3
Nighttime	2.3	3.1	3.7	4.0	3.0	4.0	4.5
Noontime	2.6 (15%)	3.9 (26%)	4.6 (23%)	4.8 (21%)	3.7 (23%)	4.7 (18%)	5.2 (16%)
Noontime+ Nighttime	2.9 (28%)	4.3 (39%)	5.1 (36%)	5.4 (35%)	4.5 (50%)	5.9 (49%)	6.7 (49%)
Weighting Average	2.5 (9%)	3.8 (21%)	4.5 (19%)	4.7 (19%)	3.7 (23%)	4.8 (21%)	5.4 (20%)

8
9

1   Table 5 Estimated SO_2 aqueous oxidation amount for the three different SO_2 diurnal variation

2   patterns, the occurrence frequency (of the three groups) weighting averaged value and the

3   relative increase compared to the nighttime peak case.

Case	SO_2 aqueous oxidized amount (ppbv day^{-1}) [Increase relative to nighttime peak case (%)]		
	Summer	Autumn	Winter
Nighttime Peak	86.5	64.2	62.4
Noontime Peak	97.5 (13%)	91.6 (43%)	77.2 (24%)
Nighttime+Noontime Peak	110.9 (28%)	99.7 (55%)	100.6 (61%)
Weighting average	93.3 (8%)	85.5 (33%)	78.8 (26%)

4

5
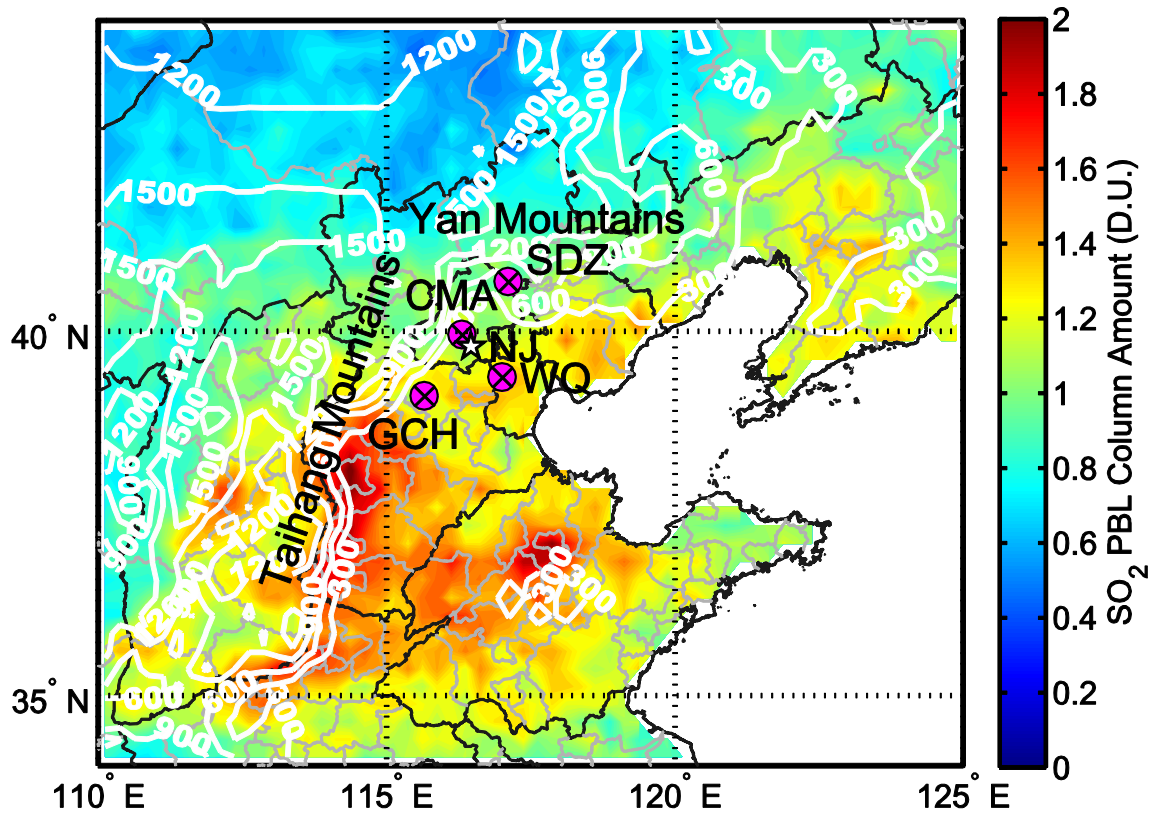
Figure 1 Location of the Shangdianzi (SDZ), China Meteorological Administration (CMA), Gucheng (GCH), Wuqing (WQ) site, the Nanjiao meteorological station (NJ) and the Yan and Taihang Mountains. The average distribution of OMI SO2 column concentration in 2009 is displayed as the shaded contour, while the white contour lines show the terrain height (m).
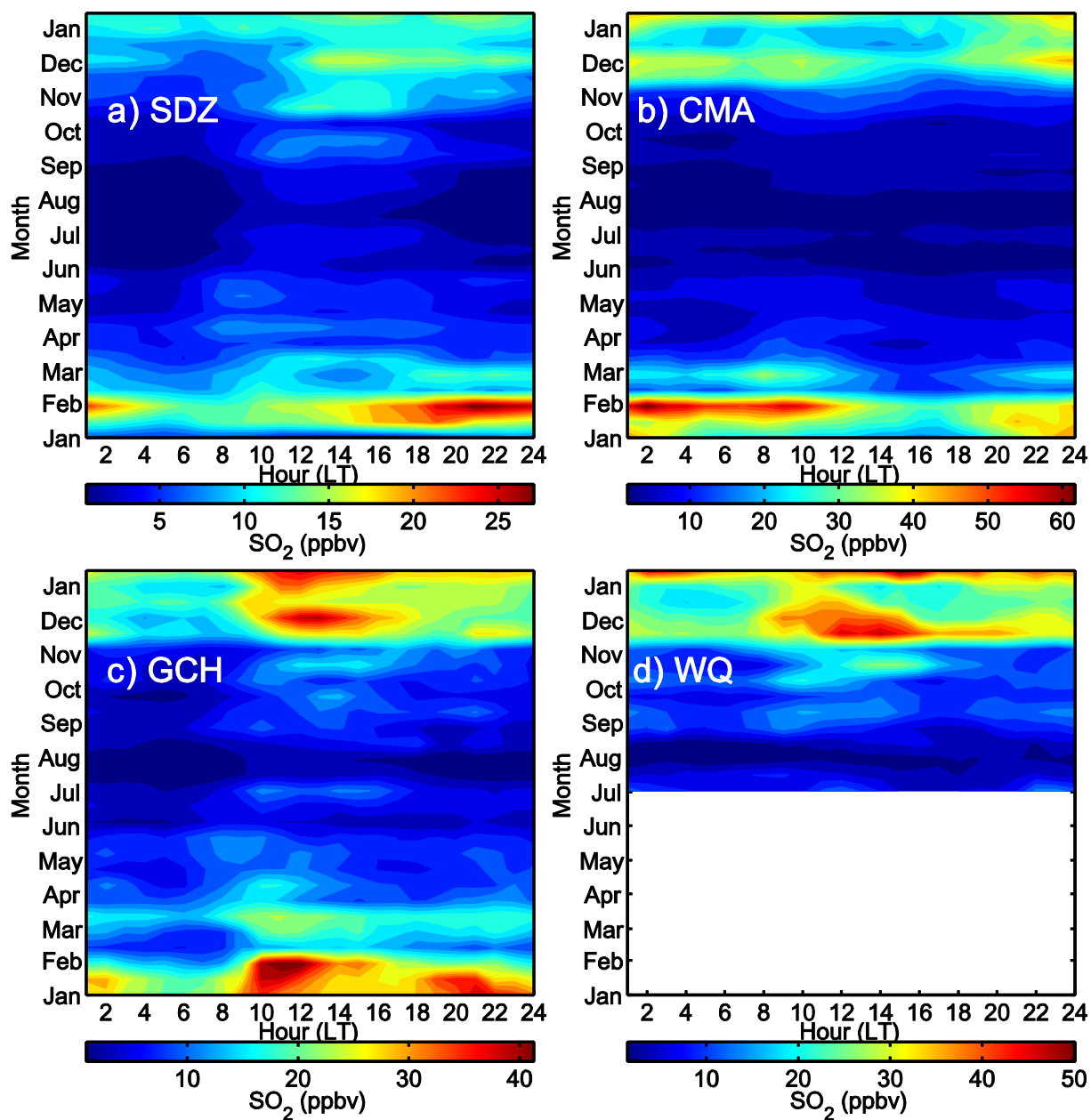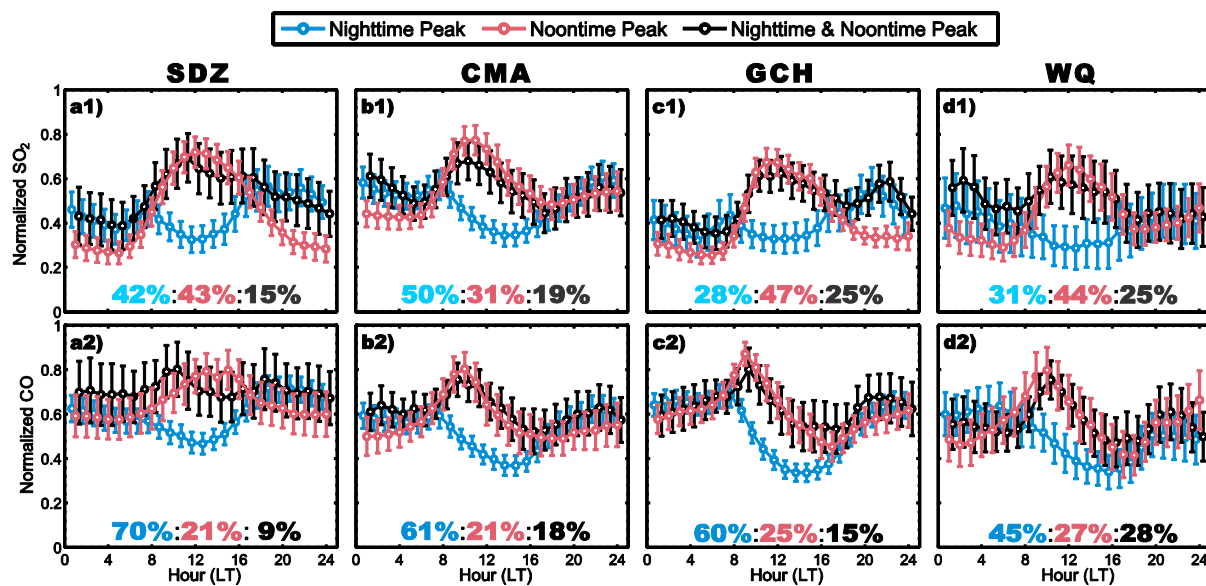
Figure 2 Diurnal and seasonal variation of SO_2 concentrations at the a) Shangdianzi, b) China Meteorological Administration, c) Gucheng and d) Wuqing site.

Figure 3 Normalized 1) SO_2 and 2) CO diurnal variation pattern for the days with peaks occurring during nighttime (blue, before 9 a.m. or after 16 p.m.), noontime(red, between 9 a.m. and 16 p.m.) and during both nighttime and noontime (black) at a) Shangdianzi, b) China Meteorological Administration, c) Gucheng and d) Wuqing station. The circle and error bar represent the average value ± 3 standard error of the mean.
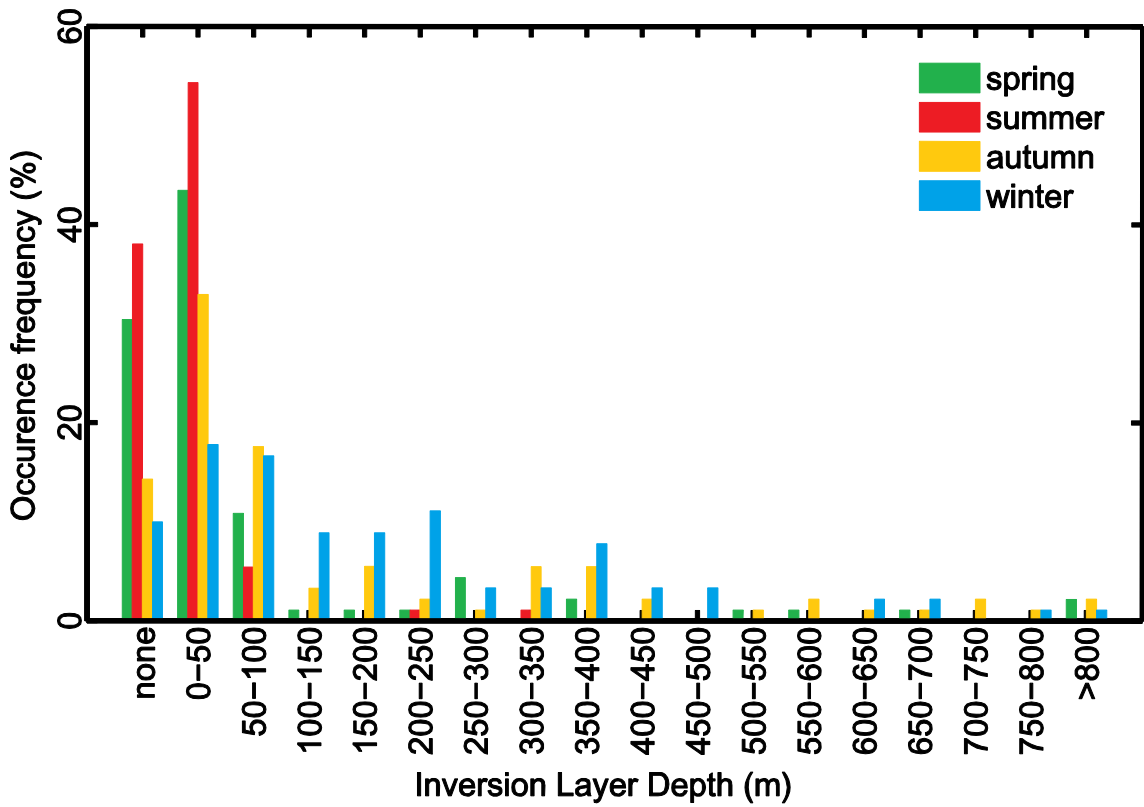
1

2   Figure 4 The occurrence frequency of different temperature inversion layer depths during spring

3   (Mar-May 2009), summer (Jun-Aug 2009), autumn (Sep-Nov 2009) and winter (Dec 2009 –
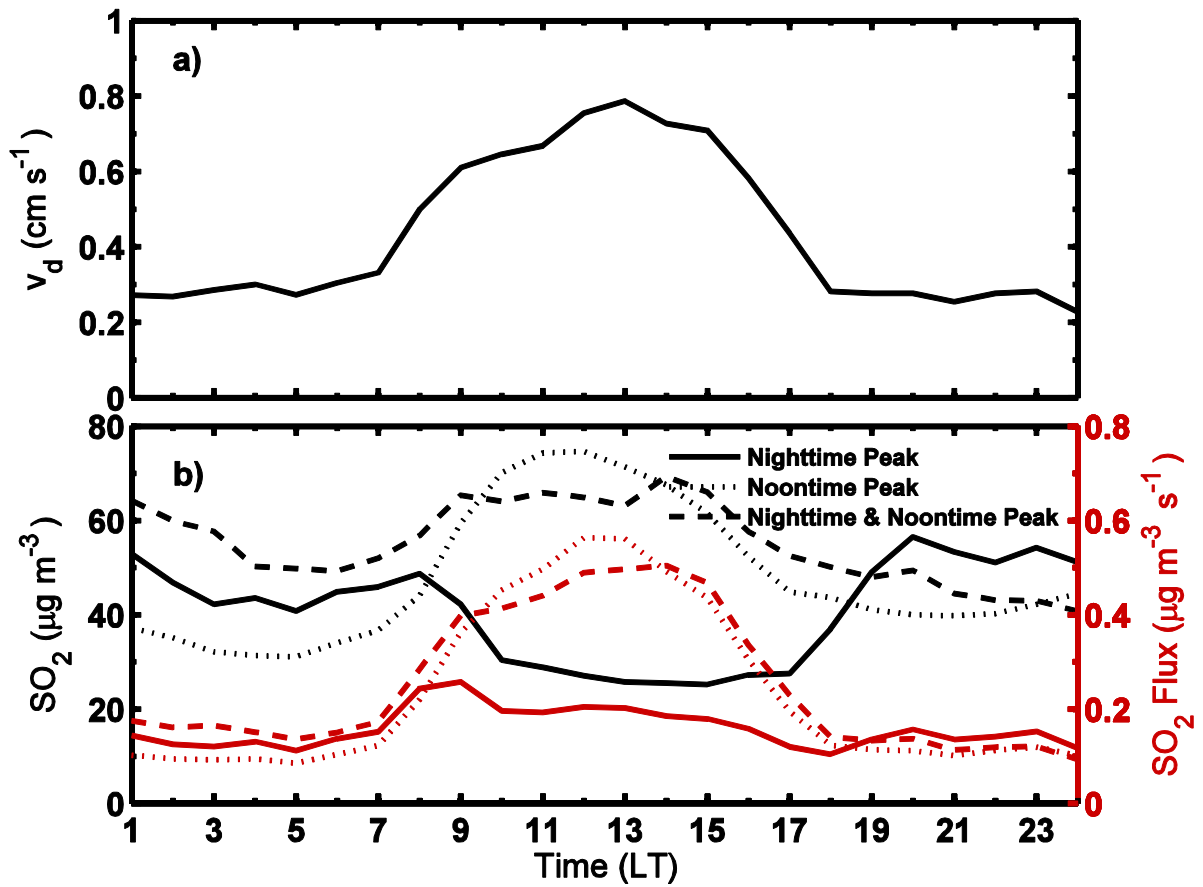
4   Feb 2010) in the 08 LT radiosonde data.

5

2
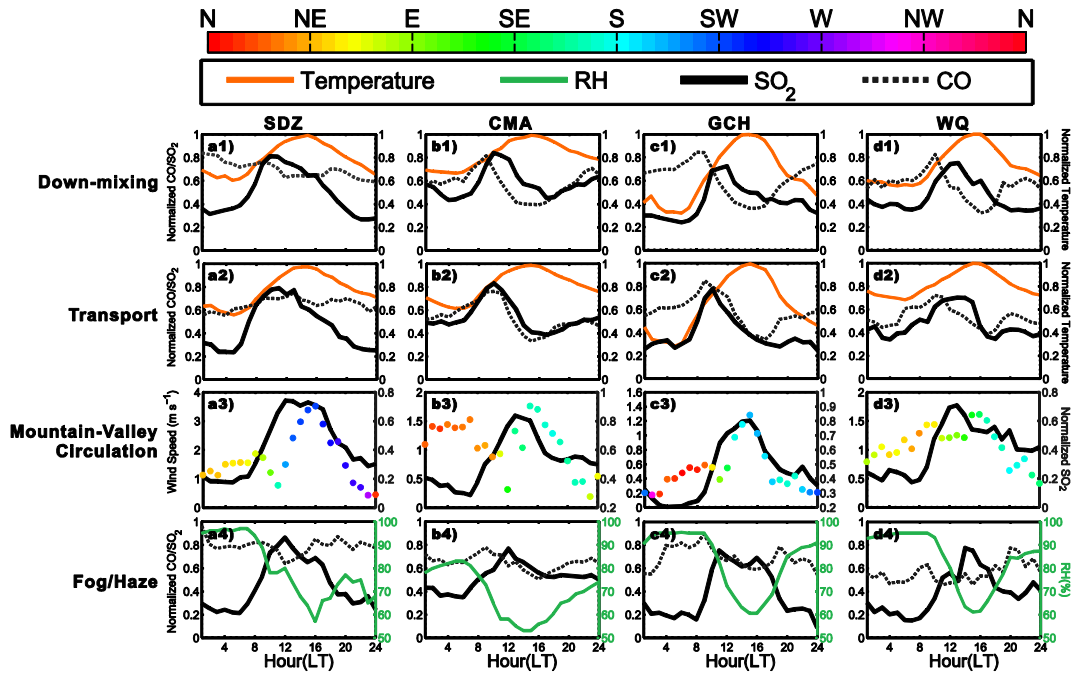
Figure 5 Averaged diurnal variation patterns for 1) the PBL down-mixing, 2) the plume transport, 3) the mountain valley breeze and 4) the fog/haze case for a) Shangdianzi, b) China Meteorological Administration, c) Gucheng and d) Wuqing.

1

2   Figure 6 a) Diurnal variation of the dry deposition velocity inferred from Tsai et al. (2010); b)

3   Calculated dry deposition fluxes (red lines) based on the three characteristic SO_2 diurnal

4   variation patterns (black lines) in Wuqing during autumn 2009.

5
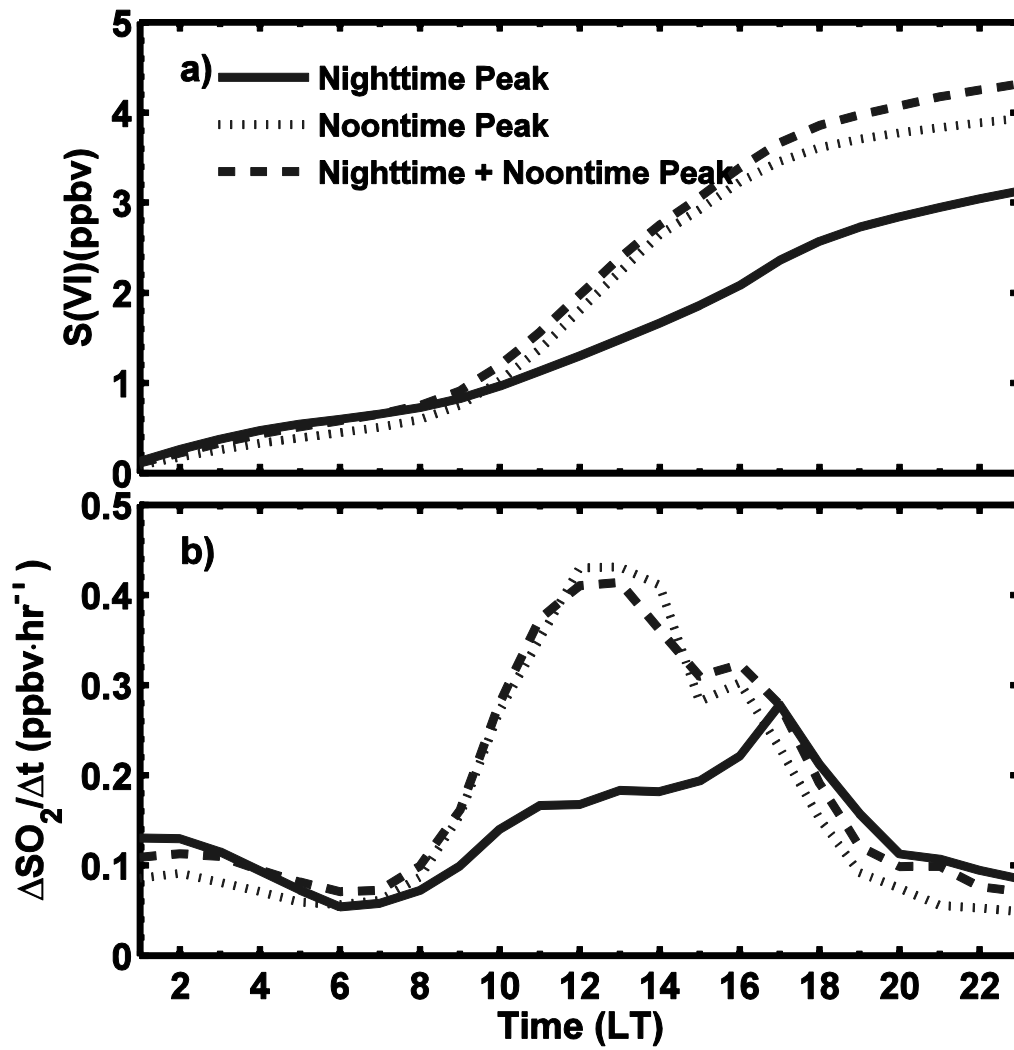
1

2 Figure 7 Simulated gas phase oxidized SO₂ a) amount and b) oxidation rates based on the three

3 characteristic SO₂ diurnal variation patterns in Wuqing during autumn 2009.

4

1
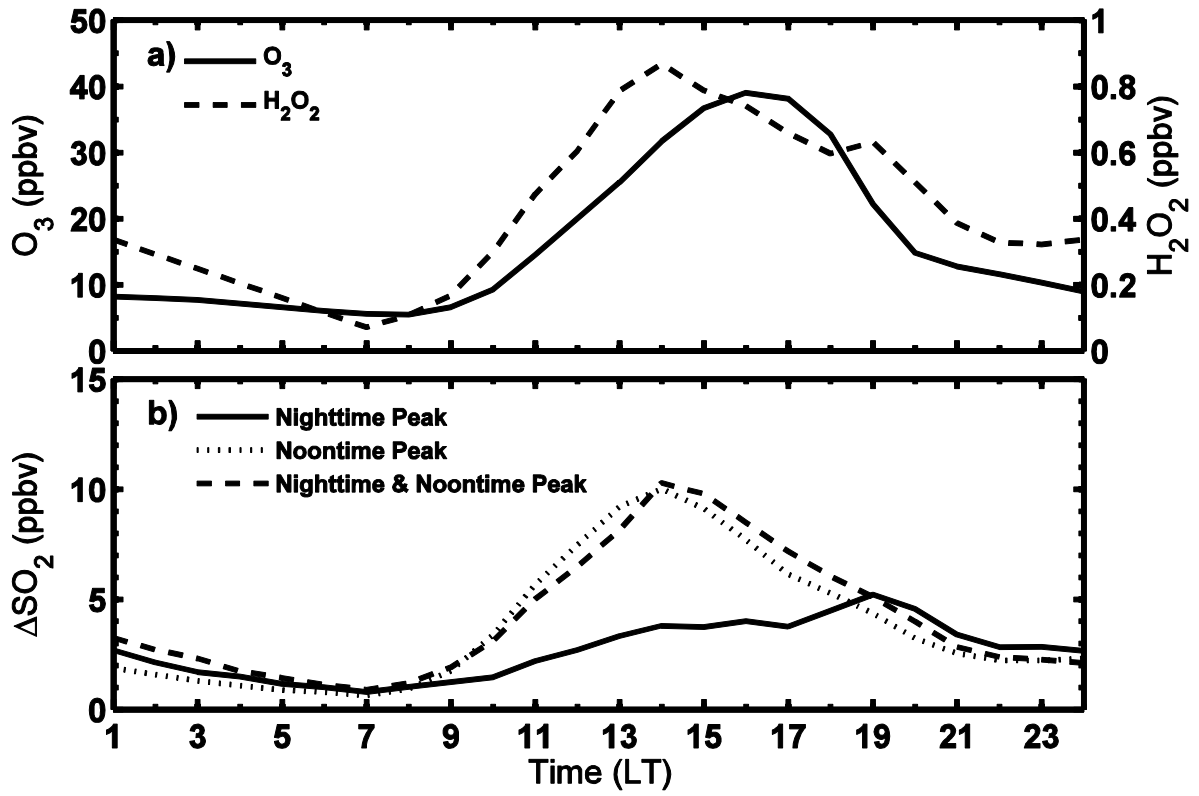
2   Figure 8 a) O_3 and H_2O_2 diurnal profiles used in the estimations; b) Estimated aqueous phase

3   oxidized SO_2 amount based on the three characteristic SO_2 diurnal variation patterns in Wuqing

4   during autumn 2009.

5